Observation of dipole-like gap solitons in self-defocusing waveguide lattices

Article *in* Optics Letters · November 2007

DOI: 10.1364/OL.32.003011 · Source: PubMed

10 authors, including:

Liqin Tang
Nankai University
67 PUBLICATIONS **536** CITATIONS
SEE PROFILE

Cibo Lou
Nankai University
71 PUBLICATIONS **803** CITATIONS
SEE PROFILE

Xiaosheng Wang
Xiangya Hospital of Central South University
32 PUBLICATIONS **872** CITATIONS
SEE PROFILE

Daohong Song
90 PUBLICATIONS **1,000** CITATIONS
SEE PROFILE

Observation of dipole-like gap solitons in self-defocusing waveguide lattices

Liqin Tang,[1] Cibo Lou,[1] Xiaosheng Wang,[2] Daohong Song,[1] Xingyu Chen,[1] Jingjun Xu,[1] Zhigang Chen,[1,2,*] H. Susanto,[3] K. Law,[3] and P. G. Kevrekidis[3]

[1]*The Key Laboratory of Weak-Light Nonlinear Photonics, Ministry of Education and TEDA Applied Physical School, Nankai University, Tianjin 300457, China*

[2]*Department of Physics and Astronomy, San Francisco State University, San Francisco, California 94132, USA*

[3]*Department of Mathematics and Statistics, University of Massachusetts, Amherst, Massachusetts 01003, USA*

**Corresponding author: zchen@stars.sfsu.edu*

Received June 6, 2007; revised July 20, 2007; accepted September 1, 2007; posted September 11, 2007 (Doc. ID 83873); published October 9, 2007

We observe dipole-like gap solitons in two-dimensional waveguide lattices optically induced with a self-defocusing nonlinearity. Under appropriate conditions, two mutually coherent input beams excited in neighboring lattice sites evolve into a self-trapped state, whose spatial power spectrum and stability depend strongly on the initial excitation conditions. Our experimental observations are compared with numerical simulations. © 2007 Optical Society of America

OCIS codes: 190.0190, 190.5330, 250.5530.

Wave propagation in optical periodic structures is known to exhibit fundamental features particular to the presence of photonic bands and forbidden gaps. Under nonlinear propagation, an optical beam can self-trap to form a gap soliton (GS) with its propagation constant residing within a photonic bandgap, in contrast with conventional discrete solitons [1,2] formed in the semi-infinite gap due to total internal reflection. Spatial GSs [3] can arise from Bloch modes in the first band [close to high-symmetry M points, i.e., the edges of the first Brillouin zone (BZ)], where anomalous diffraction is counteracted by self-defocusing nonlinearity [4–6], or the second band (close to X points), where normal diffraction is balanced by self-focusing nonlinearity [7,8]. Recently, a new bound state of GS trains has been demonstrated without *a priori* spectral or phase engineering [9], suggesting that nonlinear spectrum reshaping can lead to energy transfer between regions initially excited and unexcited in the k-space (momentum space).

In this Letter, we report the experimental demonstration of dipole-like spatial GSs in a two-dimensional (2D) optically induced "backbone" lattice [4,9] with a saturable self-defocusing nonlinearity. Our experiments show that two mutually coherent dipole-like beams can evolve into a self-trapped state. The spatial power spectra and phase structures of these dipoles are dramatically different for linear and nonlinear propagation. Our theoretical analysis shows that the stability of these high-order solitons depends strongly on the initial excitation conditions (such as relative location and phase between the two beams).

The experimental setup for our study is similar to those used earlier for the creation of optically induced lattices [10,11]. A partially spatially incoherent beam (488 nm) is generated by using a rotating diffuser. A negatively biased photorefractive crystal (SBN:60 6 mm × 10 mm × 5 mm) is employed to provide a self-defocusing nonlinearity. To generate a 2D-waveguide lattice, we use an amplitude mask to spatially modulate the otherwise uniform beam after the diffuser. The lattice (spacing ~25 μm) beam is diagonally oriented and ordinarily polarized, thus the induced waveguide arrays remain invariant during propagation. A typical lattice intensity pattern, its spatial spectrum, and the dispersion curve for the first band are illustrated in Fig. 1. An extraordinarily polarized probe beam (intensity ~6 times weaker than that of the lattice beam) is sent into a Mach–Zehnder interferometer to create a dipole-like input pattern whose phase is controlled with the piezo-transducer (PZT) mirrors. Taking advantage of the photorefractive noninstantaneous response, we monitor the linear and nonlinear transport of the probe beam simply by recording its instantaneous (before nonlinear self-action) and steady-state (after self-action) output patterns/spectra.

Our motivation is to create multipole gap lattice solitons with a defocusing nonlinearity and to illustrate the similarities and differences in comparison with their counterparts in the focusing case [12]. In particular, we study dipole-like structures (with two peaks) excited at the intensity minima (index maxima) of the 2D "backbone" lattice. For the dipole-like structure, the two intensity peaks can be in phase (IP) or out of phase (OOP), and they can be located [see Fig. 1(a)] either in the two nearest wave-

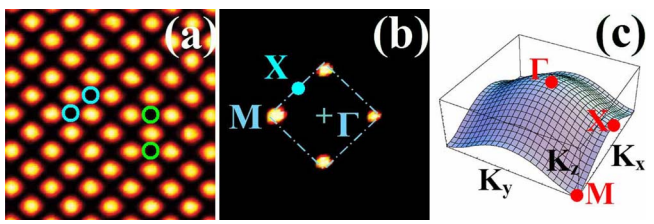

Fig. 1. (Color online) (a) Lattice pattern obtained from experiment with the two left (two right) circles marking the diagonal (vertical) excitation of the probe beam. (b) Fourier spectrum of (a) with dashed lines marking the first BZ. (c) Band structure for the first Bloch band.

guide sites (e.g., diagonal excitation along one direction of the principal axes) or in the two next nearest sites (e.g., vertical excitation along one diagonal direction of the square lattice).

First, we present our experimental results under diagonal excitation [see the two circles on the left in Fig. 1(a)]. Figure 2 shows the intensity patterns, Fourier spectra, and interferograms for both the IP case [Figs. 2(a) and 2(b)] and the OOP case [Figs. 2(c) and 2(d)]. In order to open the first gap in the defocusing lattice, a high-lattice potential is achieved by increasing the lattice intensity and the bias field (with the resulting index change for the lattice on the order of 10^{-4}). Under this lattice condition, we do not see a significant difference in intensity patterns between the linear [Figs. 2(a) and 2(c)] and nonlinear [Fig. 2(b) and 2(d)] cases simply because of the reduced coupling, although nonlinear trapping typically leads to longer "tails" for the dipole. However, remarkable differences can be seen in the spectrum and phase structure of the dipole "tails." Due to constructive phase relation, the linear spectrum of the IP dipole covers the first BZ with most of the power concentrating in the center [Fig. 2(a), middle]. Under a bias field of –1.1 kV/cm, however, the nonlinear spectrum reshapes and the energy transfers from the central region (normal diffraction) toward two lateral regions close to the two X points [where diffraction is anomalous along the y direction, as seen in Fig. 1(c)]. Because of the opposite dispersion/diffraction in two orthogonal directions at the X points in the first bandgap, the power spectrum in each side is elongated along the x direction, as the energy transfers further toward the regions close to M points where the diffraction is anomalous in both transverse directions. We visualize the phase structure of the dipole nonlinear output by taking its interference pattern with a tilted broad beam. The initial IP structure of the dipole is preserved in the central two peaks, while the tails along the dipole direction show signs of the OOP relation between adjacent peaks as the fringes tend to break and shift, as if to match the Bloch modes at the M points of the first band (OOP along the dipole direction [13]).

When the two beams exiting the interferometer are made to be OOP with each other while keeping all other experimental conditions unchanged, we also observe self-trapping of a dipole-like structure [Figs. 2(c) and 2(d)]. The OOP dipole appears to have much longer "tails" along the principal axes. Due to destructive phase relation, the linear spectrum of the diagonally excited OOP dipole covers the four M points [Fig. 2(c)]. Under nonlinear propagation, the spectrum reshapes and the energy transfers quickly to the regions close to the four M points where diffraction is anomalous [Fig. 2(d)]. It can be clearly seen that the dipole has an OOP or "staggered" phase structure not only for the central two peaks but also for any two adjacent peaks in the tails along the dipole direction [Fig. 2(d), bottom], characteristic to Bloch modes at M points of the first band [13].

These observations are compared with our numerical simulations with the initial conditions similar to those of the experiments. The model is similar to that used in [13] but here a self-defocusing nonlinearity is employed. Figure 3 shows the simulation results of the dipole-like structure under diagonal excitation for the IP case (left) and the OOP case (right), corresponding to experimental results in Fig. 2. Excellent agreement can be seen for a propagation distance up to 10 mm (i.e., our crystal length). Although we cannot observe a significant difference between linear and nonlinear propagation within our crystal length, simulations with a longer distance of 40 mm (Fig. 3, bottom panel) clearly show the self-trapping of the gap soliton states. Simulations also show that the spectrum in Fig. 3(b) tends to settle into regions close to the four M points as in Fig. 3(d), and the IP dipoles are more robust than the OOP dipoles under diagonal excitation.

Next, the dipole orientation is changed from diagonal to vertical so as to excite the two next-to-nearest waveguides [see the two green spots in Fig. 1(a)]. Results are presented in Fig. 4. In this case, the linear spectrum of the IP dipole covers the two M points in the horizontal direction, with visible excitation also in regions close to the two M points in the vertical direction [Fig. 4(a)]. Under self-defocusing nonlinearity, the power grows quickly in regions close to these four M points where diffraction is anomalous [Fig. 4(b)]. In contrast, the linear spectrum of the OOP dipole covers only the two M points in the vertical direction [Fig. 4(c)]. With the nonlinearity, the power

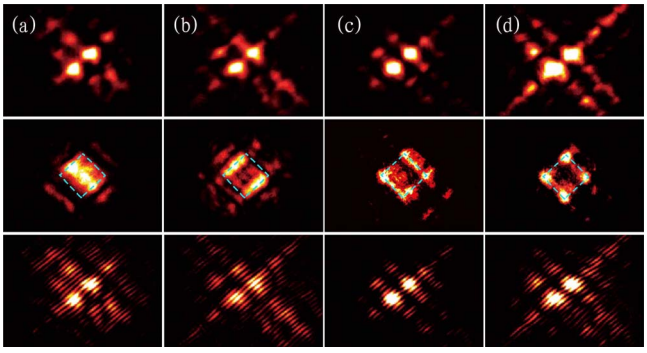

Fig. 2. (Color online) Experimental results on IP (a), (b) and OOP (c), (d) dipole-like gap solitons under diagonal excitation. Shown are output patterns (top), corresponding Fourier spectra (middle), and interferograms (bottom) for linear (a), (c) and nonlinear (b), (d) propagation.

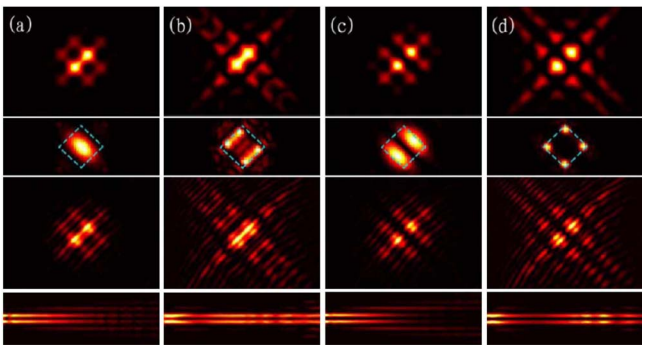

Fig. 3. (Color online) Numerical results obtained by using parameters corresponding to those of Fig. 2. Bottom row: simulation to a longer propagation distance of 40 mm (i.e., 4 times longer than the crystal length).

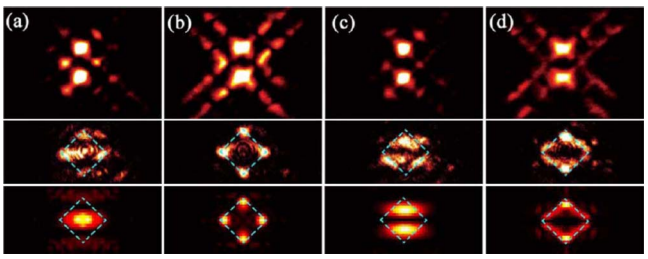

Fig. 4. (Color online) Experimental (rows 1, 2) and numerical (row 3) results on IP (a), (b) and OOP (c), (d) dipole-like gap solitons under vertical excitation. Shown are output patterns (row 1) and corresponding spectra (rows 2, 3) for linear (a), (c) and nonlinear (b), (d) propagation.

grows mainly in regions close to these two points [Fig. 4(d)], but transferring to regions close to the other two horizontal M points is clearly visible as a result of nonlinear k-space evolution [9]. Numerical results for a spectrum with the same propagation distance are shown at the bottom of Fig. 4 for comparison. Simulations to longer distances show that the OOP dipoles are more robust than the IP dipoles under vertical excitation.

Experimentally, it is a challenge to study the stability of these self-trapped dipole structures due to a limited propagation distance (crystal length). We have thus investigated this issue by linear stability analysis for the dipole GS solutions found corresponding to experimental observations. Our analysis shows that the IP nearest dipoles and OOP next-to-nearest dipoles have stability regions in defocusing lattices, whereas the OOP nearest dipoles and IP next-to-nearest dipoles are always linearly unstable. These soliton solutions and corresponding maximal growth rates [maximum real part Re(λ) of the linearization eigenvalues] as a function of the propagation constant μ is illustrated in Fig. 5, where regions of zero growth rate [max(Re(λ))=0] indicate the stability of the dipole solutions. These results show that the nearest IP dipole can be stable (for $4.2 \leqslant \mu \leqslant 4.91$) but the OOP one cannot, in sharp contrast to the self-focusing case [12]. The intuitive picture for such differences might be that in the focusing case the dipole solitons arise from modes at Γ points of the first band, which have a uniform phase, in favor of stable OOP dipole solitons, but in the defocusing case the solitons arise from modes at M points of the first band, which have a checkerboard phase structure [13], thus in favor of stable IP dipole-like GSs. Such stability properties are consistent with earlier analysis based on a staggering transformation with a discrete model [14].

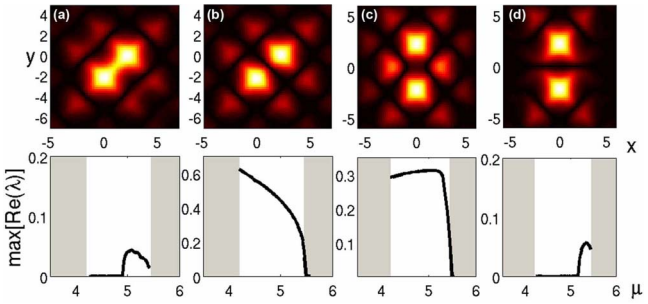

Fig. 5. (Color online) Soliton solutions (top) and stability curves (bottom) for nearest IP (a) and OOP (b), and next-to-nearest IP (c) and OOP (d) dipole gap solitons. Zero growth rates in (a), (d) indicate the stable regions of the dipole solutions.

In summary, we have demonstrated dipole-like spatial gap solitons in a 2D self-defocusing waveguide lattice. Our experimental observations are supported by theoretical analysis and numerical simulations.

This work was supported by the 973 Program, NSFC, PCSIRT, NSF, and AFOSR.

References

1. D. N. Christodoulides and R. I. Joseph, Opt. Lett. **13**, 794 (1988).
2. H. S. Eisenberg, Y. Silberberg, R. Morandotti, A. R. Boyd, and J. S. Aitchison, Phys. Rev. Lett. **81**, 3383 (1998).
3. Y. S. Kivshar, Opt. Lett. **18**, 1147 (1993).
4. J. Fleischer, M. Segev, N. Efremidis, and D. N. Christodoulides, Nature **422**, 147 (2003).
5. F. Chen, M. Stepić, C. Rüter, D. Runde, D. Kip, V. Shandarov, O. Manela, and M. Segev, Opt. Express **13**, 4314 (2005).
6. G. Bartal, O. Cohen, O. Manela, M. Segev, J. W. Fleischer, R. Pezer, and H. Buljan, Opt. Lett. **31**, 483 (2006).
7. D. Mandelik, R. Morandotti, J. S. Aitchison, and Y. Silberberg, Phys. Rev. Lett. **92**, 093904 (2004).
8. D. Neshev, A. A. Sukhorukov, B. Hanna, W. Krolikowski, and Y. S. Kivshar, Phys. Rev. Lett. **93**, 083905 (2004).
9. C. Lou, X. Wang, J. Xu, Z. Chen, and J. Yang, Phys. Rev. Lett. **98**, 213903 (2007).
10. Z. Chen and K. McCarthy, Opt. Lett. **27**, 2019 (2002).
11. H. Martin, E. D. Eugenieva, Z. Chen, and D. N. Christodoulides, Phys. Rev. Lett. **92**, 123902 (2004).
12. J. Yang, I. Makasyuk, A. Bezryadina, and Z. Chen, Stud. Appl. Math. **113**, 389 (2004).
13. D. Träger, R. Fischer, D. N. Neshev, A. A. Sukhorukov, C. Denz, W. Królikowski, and Y. S. Kivshar, Opt. Express **14**, 1913 (2006).
14. P. G. Kevrekidis, H. Susanto, and Z. Chen, Phys. Rev. E **74**, 066606 (2006).